A RADIATION SHIELDING CODE FOR SPACECRAFT AND ITS VALIDATION

J. L Shinn[1], F. A. Cucinotta[2], R. C. Singleterry[1], J. W. Wilson[1], F. F. Badavi[3], G. D. Badhwar[2], J. Miller[4], C. Zeitlin[4], and L. Heilbronn[4], R. K. Tripathi[1,5], M. S. Clowdsley[6], and J. H. Heinbockel[6]

[1]NASA Langley Research Center, Hampton, VA
[2]NASA Johnson Space Center, Houston, TX
[3]Christopher Newport University, Newport News, VA
[4]Lawrence Berkeley National Laboratory, Berkeley, CA
[5]National Research Council, Washington, DC
[6]Old Dominion University, Norfolk, VA

ABSTRACT

KEY WORDS: Spacecraft Design; Space Radiation; Radiation Shielding

The HZETRN code, which uses a deterministic approach pioneered at NASA Langley Research Center, has been developed over the past decade to evaluate the local radiation fields within sensitive materials (electronic devices and human tissue) on spacecraft in the space environment. The code describes the interactions of shield materials with the incident galactic cosmic rays, trapped protons, or energetic protons from solar particle events in free space and low Earth orbit. The content of incident radiations is modified by atomic and nuclear reactions with the spacecraft and radiation shield materials. High-energy heavy ions are fragmented into less massive reaction products, and reaction products are produced by direct knockout of shield constituents or from de-excitation products. An overview of the computational procedures and database which describe these interactions is given. Validation of the code with recent Monte Carlo benchmarks, and laboratory and flight measurement is also included.

1. INTRODUCTION

There are three sources of naturally occurring ionizing radiations which concern spacecraft designers. They are galactic cosmic rays (GCR) composed of mainly protons with ten percent

helium nuclei of very broad energy and a few percent high charge and energy (HZE) ions, solar energetic particles produced in some solar flare events composed of protons and smaller number of multiple charged ions, and particles trapped within the confines of the Earth geomagnetic field. These radiations are modified through interaction with spacecraft materials to generate the interior environment to which the astronauts or sensitive electronic devices are exposed (1). To evaluate the effect of these radiations on sensitive materials such as electronic devices or human tissue, knowledge of the specific radiation types and their physical properties at the sensitive sites are required.

The radiations are modified by atomic processes whereby energy of the primary ions is transferred to the onboard spacecraft materials resulting in ionization and excitation of the atoms within the materials (2). Secondary electrons produced from the ionization often possess large kinetic energy and are the main source of effects on the critical systems. The incident radiation fields (particle types and energies) are also modified by nuclear processes whereby primary ions of high charge and energy are fragmented into multitudes of lighter ions and neutrons (3), and light ion masses are modified by pickup and stripping reactions (4). These ions and nucleon secondaries produced from fragmentation have velocities approximately equal to that of the incident nuclei and further interact with target materials to produce target fragments as they penetrate through materials (5). The heavy components of target fragments are of very short range and capable of producing very damaging effects with highly localized ionization near sensitive sites (5, 6). The HZETRN code (7–9), accompanied by its nuclear database generating code, NUCFRG2 (3) is the only known existing code to contain all the atomic and nuclear interaction processes as described above and is adaptable in an efficient engineering design environment. Given a spacecraft geometry, the HZETRN code system can efficiently evaluate the radiation fields at a specific site within the spacecraft and estimate the radiation effects on sensitive materials, such as single-event-upsets rate (6) or biological responses (10) as have been studied previously.

The HZETRN has been under development over the past decade, beginning with development of various approximation procedures (11) in solving the Boltzmann transport equations and gradually progressing toward higher levels of sophistication in parallel with the code validation effort. Code validation is accomplished through a combined effort of laboratory measurement with high-resolution instruments (12), flight measurement with space qualified instruments (13), and comparison with Monte Carlo calculations (14, 15). The code assumes a one-dimensional straight-ahead approximation for the transport of primary ions and their secondaries which is justified on the basis that the space radiations are spatially uniform and nearly isotropic. The error from a full 3-D calculation varies as the ratio of beam divergence to the radius of curvature of spacecraft structural members squared which is normally quite small (11). The effects of lateral scattering of low energy neutrons are currently being incorporated. Atomic interactions of ions with materials are relatively well known and are carefully treated in the transport calculation with additional inclusion of straggling effect in the near future. For the nuclear database, a straight forward semiempirical fragmentation model developed in the past have now evolved into a more sophisticated version, NUCFRG2, through laboratory validation. In the following, a brief discussion of the transport methods, atomic/nuclear database, and code validation effort are given.

2. TRANSPORT METHODS

The transport equations for energetic ions are obtained by balancing the change in particle flux as they cross a small volume of materials with the gains and losses caused by nuclear collisions. The collision produces secondary ions and nucleons moving in the forward direction and low-

energy fragments of the struck target nuclei. The equations for the short-range target fragments can be easily decoupled from the projectiles and solved separately (16). The remaining projectile transport equations can be written as

$$\left[\frac{\partial}{\partial x} - \frac{1}{A_j}\frac{\partial}{\partial E}S_j(E)+\sigma_j(E)\right]\Phi_j(x,E) = \sum_k \int_E^\infty \sigma_{jk}(E,E')\ \Phi_k(x,E')\,dE'. \qquad [1]$$

where $\Phi_j(x,E)$ is the flux of ions of type j with atomic mass A_j at x moving along the x-axis at energy E in units of MeV/amu, σ_j is the corresponding macroscopic nuclear absorption cross section, $S_j(E)$is the stopping power, and $\sigma_{jk}(E,E')$ is the production cross section for type j particles with energy E by the collision of a type k particle of energy E'. The term on the left side of equation [1] containing $S_j(E)$ is a result of the continuous slowing-down approximation, whereas the remaining terms are the usual Boltzmann terms. For charge $Z > 2$, the velocity of projectile fragments can be approximated to that of the projectile (16) and equation [1] can be rewritten as

$$\left[\frac{\partial}{\partial x} - \nu_j\frac{\partial}{\partial E}S(E)+\sigma_j(E)\right]\Phi_j(x,E) = \sum_{k>j}\sigma_{jk}(E)\Phi_k(x,E) \qquad [2]$$

where ν_j which denote range-scaling parameter is equal to Z_j^2/A_j and $S(E)$ is the proton stopping power. By transforming equation [2] to an integral along the characteristic curve of that particular ion and using the perturbation theory, the solution is given as a stepping procedure with step size h in the x-direction (11)

$$\begin{aligned}\psi_j(x+h,r) = e^{-\sigma_j h}\,\psi_j(x,r+h) + \int_0^h dz\, e^{-\sigma_j z}\sum_k \sigma_{jk}\frac{\nu_j}{\nu_k}e^{-\sigma_k(h-z)} \\ \times\,\psi_k\left(x,r+\frac{\nu_j}{\nu_k}z+h-z\right)\end{aligned} \qquad [3]$$

where $\psi_j(x,r) = S(E)\Phi_j(x,E)$ with r being the residual range of proton given by $r(E) = \int_0^E \frac{dE'}{S(E')}$. Equation [3] is accurate to order h^2 and is further approximated, to $O\left[(\nu_k-\nu_j)h\right]$, as

$$\psi_j(x+h,r) = e^{-\sigma_j h}\,\psi_j\left(x,r+\nu_j h\right) + \sum_k \sigma_{jk}(r)\left(\frac{e^{-\sigma_j h} - e^{-\sigma_k h}}{\sigma_k - \sigma_j}\right) \times \psi_k\left(x,r+\nu_j h\right) \qquad [4]$$

Equation [4] provides the propagating algorithm for the heavy ions. The corresponding propagating procedure for helium and nucleons ($Z \leq 2$) is given as

$$\psi_j(x+h,r) = e^{-\sigma_j(r)h}\psi_j\left(x,r+\nu_j h\right) + \sum_k \int_{r+\nu_j h/2}^{\infty} e^{-\left[\sigma_j(r)+\sigma_k(r')\right]\frac{h}{2}} \times \psi_k\left(x,r'+\nu_k\frac{h}{2}\right) dr'\,\overline{F}_{jk}\left(r,\nu_j,r'\right) + O\left(h^3\right) \qquad [5]$$

where

$$\overline{F}_{jk}\left(r,\nu_j h,r'\right) = \int_0^h \bar{f}_{jk}\left(r+\nu_j z,r'\right) dz \qquad [6]$$

where $\bar{f}(r,r')$ is the transformed differential cross section given by $\bar{f}(r,r') = S(E)\,\sigma(E,E')$. Further approximation in evaluating the double integrals in equation (5) is given in references 17 and 18. Equations [4] and [5] are the bases for HZETRN code and are solved by space marching procedures with incident radiation fields as boundary conditions. The coefficients appearing in equation [1] are related to the atomic and nuclear processes by which the particle fields are modified and are strongly dependent on the particle type, the energy and the medium. Thus, the database required for GCR transport calculations is enormous.

3. ATOMIC AND NUCLEAR DATABASE

In propagating the ions through shield materials, microscopic variations of secondary electrons emanating from the ion path as the result of atomic interaction are neglected in the continuous slowing down approximation. The related coefficient to this approximation, known as stopping power has been well studied and documented (19–21). The stopping power generated for HZETRN follows the approach of Ziegler at low energies with some modifications to Zieglers' parameters, modifications at higher energies to the shell corrections (11), inclusion of density effects (22), and cutoff factor (23) at high energies. Recent comparisons of stopping power and range calculated from various existing codes (including those from HZETRN) for selected ions and materials over the applicable energy range indicate good agreement to within one percent (24). However, to evaluate the response of a sensitive element due to ionization of a passing ion, the microscopic distribution of secondary electrons must be known. A *radial dose model* which describes the electron distribution was developed (25) based on the model of Kobetich and Katz (26) with added improvements in electron transmission and angular dependence of electron ejection. This model has been successfully used in estimating biological injury (10), CCD

(charge coupled device) response (27), and SEU (single event upset) rates in Shuttle computers (6).

Improving the nuclear database has been one of the major tasks in HZETRN code development. Due to limited accelerator beam time, it is impossible to make experimental determination of the nuclear database for all the combinations of reaction species, projectile energies, and secondary particle types. Nuclear-reaction modeling is required in bridging the gap, to validate and extrapolate laboratory measurements. The latest nuclear models for generating the nuclear fragmentation database in the HZETRN are the semiempirical NUCFRG2 code (3) and the quantum multiple scattering fragmentation QMSFRG code (28) which is still under development. These two models are being tested with a consistent set of fragmentation cross sections recently measured (29) at Brookhaven National Laboratory (BNL) AGS accelerator for 1.05 GeV/nucleon iron beam incident on various nuclei (H, C, Al, Cu, and Pb) as shown in Figures 1 and 2. The data are limited to fragments with charge greater than 12 with lighter fragments left unresolved. There is a slight overestimate by NUCFRG2 model for the larger charge removal processes which is related in part to the uncertainty in the excitation spectra of intermediate states in the fragmentation process. It is also shown that the QMSFRG model is superior to the NUCFRG2 in resolving the odd-even effect in the elemental distribution seen in the experimental data although QMSFRG overestimates for the low charge removal due to the neglect of cluster knockout processes. Inclusion of nuclear structure effects into the QMSFRG for clustering will rectify this problem. QMSFRG will ultimately replace semiempirical fragmentation models in the long run.

Total absorption cross sections have recently been updated following the development of universal parameterization by Tripathi et al. (30, 31) based on a modified Bradt-Peters form (32). The universal parameterization provides accurate predictions for any given system of ion-ion or neutron-ion collisions for the entire energy range from 1 MeV to high energies by introducing the physical processes of the collision into the parameters. At low energies, the cross section is modified by Coulomb interaction for ion-ion collision and by the optical potential at the surface for neutron-ion collision. At higher energies, the effects of Pauli blocking are important. With these physical processes added, the model has been tested with all the available data for projectiles of proton (and neutron) through krypton and targets of helium through bismuth for the entire energy range and is found to give excellent results. An example of these improvements is shown in Figure 3 indicating the results by Tripathi et al. (31) is in much better agreement with experimental data than any of the prior models (33, 34) for neutron - aluminum collision.

4. FLIGHT VALIDATION

Spaceflight radiation experiments provide an integral test of external environmental model, transport function through realistic shielding, and prediction of detector response. Thus, validation of the HZETRN requires certain degree of confidence in each of these areas. The galactic cosmic ray model has been improved over the recent years to take into account of realistic solar modulation as related to Climax neutron monitor data (35, 36). Trapped radiation, which is important for lower earth orbit in the case of Shuttle or International Space Station is also under major revision (37) and a corrected version of the AP-8 model (38) is currently being used. To model the transport function through realistic shielding not only requires design software to represent the spacecraft structure and material distribution, but also requires accurate transport solution algorithms and nuclear database, with the latter being validated through laboratory experiments as described in the previous section. Active instruments such as tissue equivalent proportional counters (TEPCs), particle telescope, or SEU-sensitive devices flown on the Shuttle

are useful in separating the contributions of galactic cosmic rays from that of trapped radiations (39) and require a separate treatment for the response of individual instrument due to differences in their instrument characteristics. Adequate response model for passive detectors such as CR-39 has also been shown to be important in resolving the difference between flight data obtained in D1 mission (an European payload mission on Shuttle at 324 km, 57-degree orbit) and HZETRN calculation (6). The significance of modeling the loss of data for very short-range particles due to etching process of CR-39 is demonstrated in Figure 4.

Recently, an analytic model was developed to predict the response of a micron-size tissue equivalent proportional counter (TEPC) used in the Shuttle experiment to take into account of the randomness due to energy loss straggling and detector chordlength distribution and to treat the problem of stopping ions (enders) and varying track width (40). This model, which has been verified (40) by comparing with Monte Carlo results given in the literature and with laboratory beam experiments, is used in the flight validation results presented herein. Figure 5 shows the GCR differential lineal energy (energy deposit per unit pathlength) and LET (linear energy transfer or stopping power) spectra for STS-56, a Shuttle flight in a 57-degree inclined orbit. The data are obtained by a TEPC located in the payload bay (41). The HZETRN result is post-processed with an accurate representation of Shuttle geometry which is predominantly aluminum. The resulting spectra with and without consideration of detector response are shown as the lineal energy and LET flux, respectively. Although the configuration of the detector head is designed to resolve some details of an LET spectrum, it is seen that the randomness due to energy loss straggling and detector chord length distribution smears out the sharp peaks as seen in the figure. Additional comparisons for TEPC measurement are shown in Figures 6(a) and 6(b) using the STS-57 flight results for GCR and trapped protons. The corrected trapped proton model appears to provide good results except in the region above 70 keV/μm indicating possible inaccuracy in the energy distribution of the AP-8 model. Also, there seems to be a systematic detection deficiency at the lowest TEPC channel and an underestimate for GCR below 2 keV/μm. Otherwise, the agreement is good and an improvement to HZETRN with addition of pions, kaons and electromagnetic cascades may further improve the results below the 2 keV/μm region for the GCR spectrum. Note that the addition of these species will not change the results for trapped protons which are already in good agreement with the data for the low lineal energy range.

Particle telescopes detect incident ions in limited solid angles and are useful in determining the directional distribution of trapped protons (42). They can also be specially designed to separate light ion species detected in the space environment as have been done by Badhwar et al. (13) in the Shuttle experiments. The measured low energy spectra of the light ions (*p, d, t, h,* and α) contributed from GCR provide experimental evidence to the secondary particle production as generated by the nuclear interaction of incident GCR with the Shuttle shielding materials since the geomagnetic cutoffs prevent primaries of this energy regime from penetrating to the low latitudes. Figure 7 shows the comparison of measured proton energy spectrum with the calculated HZETRN results. Reasonably good agreement is seen for protons; however, the code had to be modified to include pickup and knockout processes (28) to achieve better agreement for all other light ions. Figure 8 shows the measured deuteron spectrum in comparison with the original and modified HZETRN calculations to indicate the significance of these improvements.

5. IMPROVED NEUTRON TRANSPORT AND VALIDATION

The interaction of high energy space radiation with spacecraft materials generates a host of secondary particles, some, such as neutrons, are even more biologically damaging and

penetrating than the original primary ions. In common with gamma rays, neutrons carry no charge and therefore cannot interact with matter by means of Coulomb force, which dominates the energy loss mechanism for charged particles and electrons. Energetic neutrons can travel many inches of matter without any type of interaction and thus can be totally invisible to a detector of common size. A candidate instrument for detecting the full spectrum of neutrons is a set of Bonner spheres with various sizes of moderators requiring a rigorous analysis procedure following the data acquisition process (43). Thus, the limit in mass and weight requirement in space can present difficulties in using appropriate flight instrumentation and providing a meaningful flight validation of neutron component in HZETRN.

One of the viable means of validating the transport of neutron components within HZETRN is through Monte Carlo simulation of the incident proton fluence. Only the specific multiply charged production processes are ignored in this comparison. Previous validation work (15) using Monte Carlo calculation as a benchmark for nucleon spectra has revealed the deficiency in the treatment of low energy neutrons in HZETRN. The problem lies in the crudeness of the interaction cross sections (11) and inadequacy of the transport procedures, especially in the elastic scattering processes. The neutron elastic cross sections are large below several MeV and the short mean free paths result in many rescattering events. The original HZETRN adequately evaluates the propagation of ions and high-energy neutrons but special methods are required to evaluate the low energy neutron spectrum. Specialized procedures have been recently developed by one of us (MSC) to allow the improved estimates of the neutron fluence spectra within spacecraft materials. A first order account of the angular dependence of the low energy neutron environment are included as forward and backward propagating components within a more accurate representation of the neutron slowing process. Figure 9 shows comparisons of the original and improved (1- directional and 2- directional) HZETRN calculations with the Monte Carlo (MCNPX) code (44) results for the neutron fluence at the location of 30 g/cm^2 in water behind 100 g/cm^2 aluminum shield exposed to February 1956 solar flare. One can see from the figure that a greatly improved procedure for elastic scattering is available and future improvements must come in improved representation of the low energy inelastic transport processes and improvements in the cross section database used in the code. Note that the procedure used to obtain the Monte Carlo results here is the same as described in reference 15 and is approximate so that the results can be obtained within a reasonable turn-around time. It is difficult to imagine, from this experience, that the Monte Carlo codes are suitable for use in a complete engineering analysis for space radiation effects since the calculations here are only for one radiation species and for a simple geometry.

6. CONCLUDING REMARKS

The steps towards developing a transport code for radiation analysis of future missions from the input database, transport procedures, to instrumentation response have been discussed. We have shown that the nuclear reaction database for iron ion fragmentation is in reasonable agreement with the limited experimental measurements. The NUCFRG2 model gives a slight overestimate of the larger mass removal while QMSFRG overestimates for low charge removal processes. Improvements in QMSFRG will result in the treatment of the details of the mixed state structure of the groundstate wavefunctions of the incident ion. Improved absorption cross sections have resulted from the analysis of the interaction systematics of Tripathi et al. Testing of the environmental models, the vehicle geometry models, the transport procedures, the transport database, and detector response to the local charged particle environment as an integrated system in defining the environment onboard spacecraft is given by the flight data comparisons. So far, tests have been made within the Shuttle and mainly with the aluminum database. In this case,

good agreement is obtained for STS-56 and STS-57 comparisons using the TEPC except for lineal energies below about 2 or 3 keV/micron. Using the time-resolved spectra for GCR and trapped components separately reveal the GCR result to be the main cause of the disagreement and is probably due to the lack of pion production in the transport code. The telescope measurements on STS-48 indicate that the production and propagation of light ions from GCR interactions in the Shuttle aluminum structure are reasonably represented in the code. The CR-39 data from the D1 mission of spacehab indicate some of limitations of the CR-39 in detecting local LET spectra and agreement is only achieved when the post flight processing of the foils are accounted for. Otherwise large differences between calculated LET spectra and "measured" LET spectra remain for that mission. Indications are that the computations of HZETRN are more reliable than this particular technique in evaluation of LET contributions in this range. Recent advances in computational procedures for neutrons give far more realistic low energy neutron spectra. Since no instrument has yet been flown to test the full neutron range, we have used state-of-the-art Monte Carlo codes to test the production and propagation of neutrons by proton initiated reactions. Vast improvements are validated by the comparisons so that an improved neutron nuclear database is required for an in-depth comparison in the future.

7. REFERENCES

1. J. W. Wilson, L. W. Townsend, J. L. Shinn, F. A. Cucinotta, R. C. Costen, F. F. Badav and S. L. Lamkin, "Galactic cosmic ray transport methods: past, present, and future,"Adv. Space Res., 14, 841 (1994).

2. F. A. Cucinotta, R. Katz, J. W. Wilson, R. D. Dubey, "Radial dose distributions in the delta-ray theory of track structures," In: Proceedings of Two Center Effects in Ion-atom Collisions—AIP Conference Proceedings, vol. 362, pp. 245–265; 1996.

3. J. W. Wilson, J. L. Shinn, L. W. Townsend, R. K. Tripathi, F. F. Badavi, and S. Y. Chun, "NUCFRG2: A semiempirical nuclear fragmentation model," Nucl. Inst. Methods, B94, 95, (1995).

4. F. A. Cucinotta, L. W. Townsend, J. W. Wilson, J. L. Shinn, G. D. Badhwar, R. R. Dubey, "Light ion components of the galactic cosmic rays—Nuclear interactions and transport theory," Adv. Space Res., 17, 77, (1995).

5. F. A. Cucinotta, J. W. Wilson, J. L. Shinn, F. F. Badavi, G. D. Badhwar, "Effects of target fragmentation on evaluation of LET spectra from space radiations: Implications for space radiation protection studies," Radiat. Meas., 26, 923, (1996).

6. J. L. Shinn, F. A. Cucinotta, J. W. Wilson, G. D. Badhwar, P. M. O'Neill, F. F. Badavi, "Effects of target fragmentation on evaluation of LET spectra from space radiations in low earth orbit (LEO) environment—Impact on SEU predictions," IEEE Trans. Nucl. Sci., 42, 2017, (1995).

7. J. W. Wilson, F. F. Badavi, F. A. Cucinotta, J. L. Shinn, G. D. Badhwar, R. Silberberg, C. H. Tsao, L. W. Townsend, and R. K. Tripathi, "HZETRN: Description of a Free-Space Ion and Nucleon Transport and Shielding Computer Program," NASA TP-3495, 1995.

8. F. A. Cucinotta, J. W. Wilson, J. L. Shinn, R. K. Tripathi, K. M. Maung, F. F. Badavi, R. Katz, R. R. Dubey, "Computational procedures and database development," in *Shielding Strategies for Human Space Exploration*, NASA CP-3360, pp. 153–211, 1997.

9. J. L. Shinn, S. John, R. K. Tripathi, J. W. Wilson, L. W. Townsend and J. W. Norbury, "Fully energy dependent HZETRN (A galactic cosmic-ray transport code)," NASA TP-3242, 1993.

10. F. A. Cucinotta, J. W. Wilson, M. R. Shavers, and R. Katz, "Effects of track structure and cell inactivation on the calculation of heavy ion mutation rates in mammalian cells, " Int. J. Radiat. Biol., 69, (5), 593, (1996).

11. J. W. Wilson, L. W. Townsend, W. Schimmerling, G. S. Khandelwal, F. Khan, J. E. Nealy, F. A. Cucinotta, L. C. Simonsen, J. L Shinn, and J. W. Norbury, "Transport methods and interactions for space radiations," NASA RP-1257, 1991.

12. C. J. Zeitlin, K. A. Frankel, W. Gong, L. Heilbronn, E. J. Lampo, R. Leres, J. Miller, and W. Schimmerling, "A modular solid state detector for measuring high energy heavy ion fragmentation near the beam axis," Rad. Meas., 23, (1), 65, (1994).

13. G. D. Badhwar, J. U. Patel, F. A. Cuccinotta, and J. W. Wilson, "Measurements of the secondary particle energy spectra in the Space Shuttle," Rad. Meas., 24, 129, (1995).

14. J. L. Shinn, J. W. Wilson, J. E. Nealy, and F. A. Cucinotta, "Comparison of dose estimates using the buildup-factor method and a baryon transport code (BRYNTRN) with Monte Carlo results," NASA TP-3021, 1990.

15. J. L. Shinn, J. W. Wilson, M. A. Lone, P. Y. Wong, and R. C. Costen, "Preliminary estimates of nucleon fluxes in a water target exposed to solar-flare protons: BRYNTRN versus Monte Carlo code," NASA TM-4565, 1994.

16. J. W. Wilson, "Analysis of the Theory of High Energy Transport," NASA TN D-8381, 1977.

17. S. L. Lamkin, G. S. Khandelwal, J. L. Shinn, J. W. Wilson, "Space proton transport in one dimension," Nucl. Sci. Eng., 116, 291, (1994).

18. Cucinotta, "Calculations of cosmic ray helium transport in shielding materials," NASA TP-3354, 1993.

19. J. F. Ziegler, J. P. Biersack, and U. Littmark, "The stopping and range of ions in solids," The Stopping and Ranges of Ions in Matter, 1, J. F. Ziegler, ed., Pergamon Press, 1985.

20. F. Hubert, R. Bimbot, and H. Gauvin, "Range and stopping power tables for 2.5-500 MeV/Nucleon heavy ions in solids," Atomic Data and Nucl. Data Tables, 46, (1), 1, (1990).

21. Joseph F. Janni, "Proton range-energy tables, 1 keV-10 GeV—energy loss, range, path length, time-of-flight, straggling, multiple scattering and nuclear interaction probability," Atomic Data & Nucl. Data Tables, 27, Part 1 and Part 2, 1982.

22. J. L. Shinn, H. Farhat, F. F. Badavi, and J. W. Wilson, "Polarization correction for ionization loss in a galactic cosmic ray transport code (HZETRN),"NASA TM-4443, 1993.

23. U. Fano, "Penetration of protons, alpha particles, and messons," Annual Review of Nuclear Science, 13, Emilio Segre ed., Annual reviews, Inc., 1963, pp. 1–66.

24. H. Tai, H. Bichsel, J. W. Wilson, J. L. Shinn, F. A. Cucinotta, and F. F. Badavi, "Comparison of stopping power and range database for radiation transport study," NASA TP-3644, 1997.

25. F. A. Cucinotta, R. Katz, J. W. Wilson, and R. R. Dubey, "Heavy ion track-structure calculations for radial dose in arbitrary materials," NASA TP-3497, 1995.

26. E. J. Kobetich, and R. Katz, "Width of heavy-ion tracks in emulsion," Phys. Rev., 170, (2), 405, (1968).

27. L. C. Simonsen, "Evaluation of a charged coupled device (CCD) for use as a nuclear charged particle detector for space applications," Ph. D. Dissertation, University of Virginia, 1997.

28. F. A. Cuccinotta, J. W. Wilson, R. K. Tripathi, and L. W. Townsend, "Microscopic fragmentation model for galactic cosmic ray studies," Submitted to Adv. Space Res.

29. C. Zeitlin, L. Heilbronn, J. Miller, S. E. Rademacher, T. Borak, T. R. Carter, K. A. Frankel, W. Schimmerling and C. E. Stronach, "Heavy fragment production cross sections from 1.05 GeV/nucleon ^{56}Fe in C, Al, Cu, Pb and CH2 targets," Phys. Rev., C56, 388, (1997).

30. R. K. Tripathi, F. A. Cucinotta, and J. W. Wilson, "Accurate universal parameterization of absorption cross sections," Nucl. Instr. and Meth., B117, 347, (1996).

31. R. K. Tripathi, J. W. Wilson, and F. A. Cucinotta, "Accurate universal parameterization of absorption cross sections II—neutron absorption cross sections," Nucl. Instr. and Meth., B129, 11, (1997).

32. H. L. Bradt, and B. Peters, "The heavy nuclei of the primary cosmic radiation," Phys. Rev., 77, 54, (1950).

33. J. W. Wilson, L. W. Townsend, W. W. Buck, S. Y. Chun, B. S. Hong, and S. L. Lamkin, "Nucleon-nucleus interaction data base—total nuclear and absorption cross sections," NASA TM-4053, 1988.

34. J. R. Letaw, R. Silberberg, C. H. Tsao, "Proton-nucleus total inelastic cross sections—an empirical formula for E greater than 10 MeV," Astrophys. J. Suppl. Ser., 51, 271, (1983).

35. G. D. Badhwar and P. M. O'Neill, "An improved model of galactic cosmic radiation for space exploration missions," Nucl. Tracks Radiat. Meas., 20, (3), 403, (1992).

36. R. A. Nymmik, M. I. Panasyuk, T. I. Pervaja, and A. A. Suslov, "A model of galactic cosmic ray fluxes," Nucl. Tracks Radiat. Meas., 20, 427, (1992).

37. S. L. Huston and K. A. Pfitzer, "A new model for the low altitude trapped proton environment," IEEE Trans. Nucl. Sci., 45, 2972, (1998).

38. E. J. Daly and H. D. R. Evans, "Problems in radiation environment models at low altitudes," Memorandum ESA/ESTEC/WMA/92-067/ED, 1993.

39. G. D. Badhwar, A. Konradi, A. Hardy, and L. A. Braby, "Active dosimetric measurements on Shuttle flights," Nucl. Tracks Radiat. Meas., 20, 13, (1992).

40. J. L. Shinn, G. D. Badhwar, M. A. Xapsos, F. A. Cucinotta, and J. W. Wilson, "An analysis of energy deposition in a tissue equivalent proportional counter onboard the Space Shuttle," submitted to Radiat. Meas.

41. G. D. Badhwar, F. A. Cuccinotta, L. A. Braby, and A. Konradi, "Measurements on the shuttle of the LET spectra of galactic cosmic radiation and comparison with the radiation transport model," Rad. Res., 139, 344, (1994).

42. J. Kopp, R. Beaujean, G. Reitz, and J. U. Schott, "Radiation measurements on manned space flights," Presented at the 32nd Scientific Assembly of COSPAR, Nagoya, Japan, paper F2.1 - 0010, July 12–19, 1998.

43. P. Goldhagen, "Overview of aircraft radiation exposure and recent ER-2 measurements," Proceedings of the thirty-fourth annual meetings of the National Council on Radiation Protection and Measurements, Arlington, VA, April 1–2, 1998, Proceedings No. 20, in press.

44. H. G. Hughes, R. E. Prael, and R. E. Little, "MCNPX—The LAHET/MCNP code merger," LA-UR-97-4891, Los Alamos National Laboratory, Los Alamos, NM, April 22, 1997.

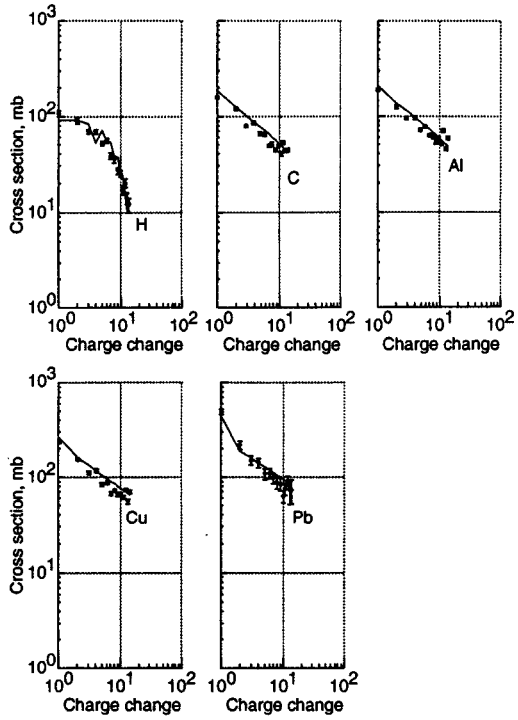

Figure 1. Charge-changing cross sections for ΔZ from -1 to -14 for 1.05 GeV/nucleon ^{56}Fe incident on H, C, Al, Cu, and Pb targets. The solid lines are prediction from NUCFRG2.

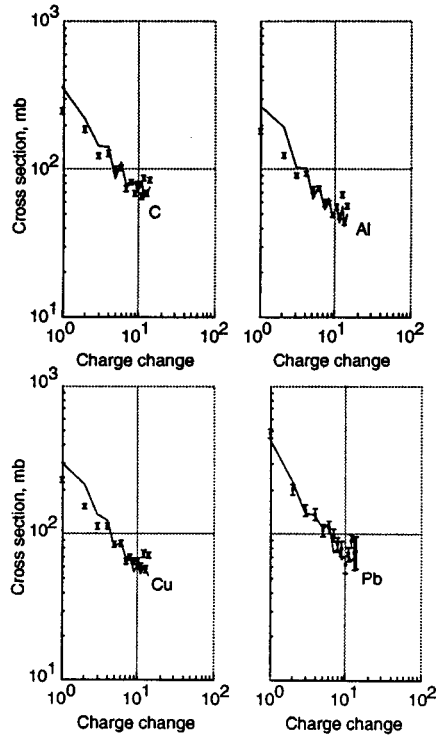

Figure 2. Charge-changing cross sections for ΔZ from -1 to -14 for 1.05 GeV/nucleon ^{56}Fe incident on C, Al, Cu, and Pb targets. The solid lines are prediction from QMSFRG.

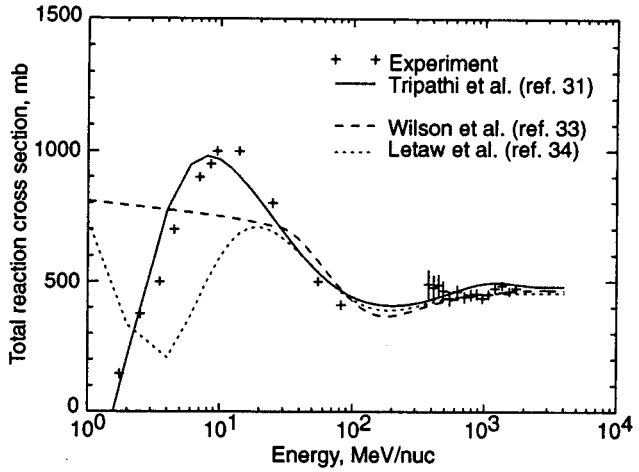

Figure 3. Total absorption cross sections for n + $^{27}_{13}$Al as a function of neutron energy.

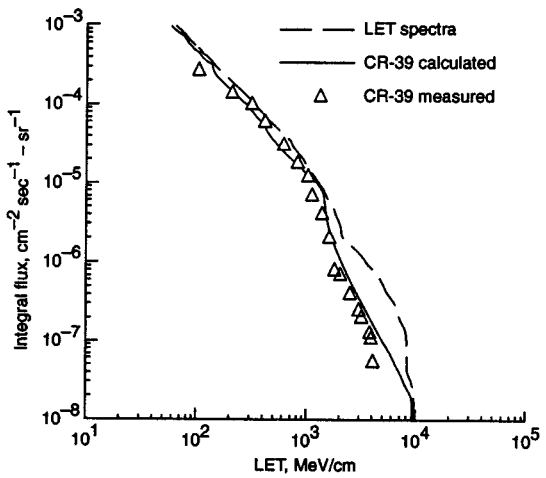

Figure 4. Calculated LET spectra, predicted CR-39 response, and measured CR-39 response for D1 mission.

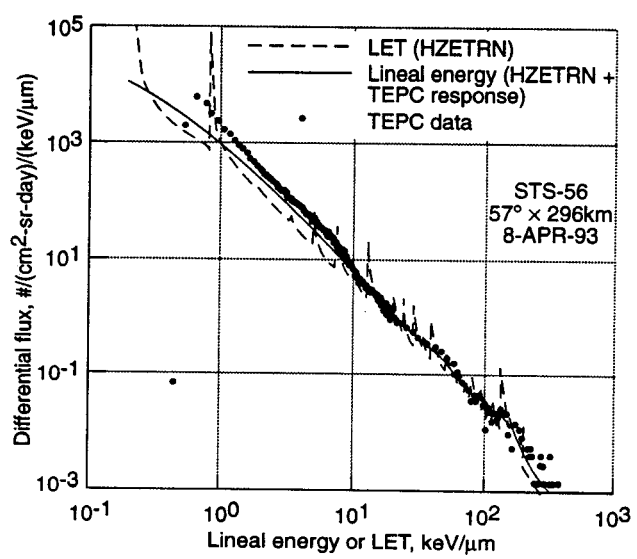

Figure 5. GCR differential LET or lineal energy spectra, in comparison with TEPC data for a 57-degree Shuttle flight.

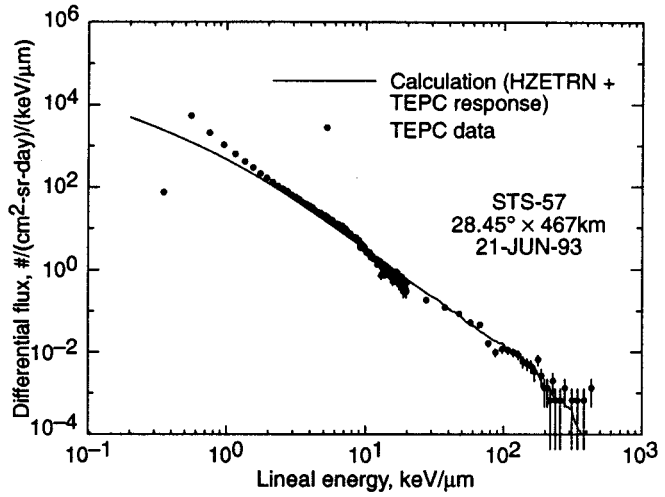

(a) GCR contribution

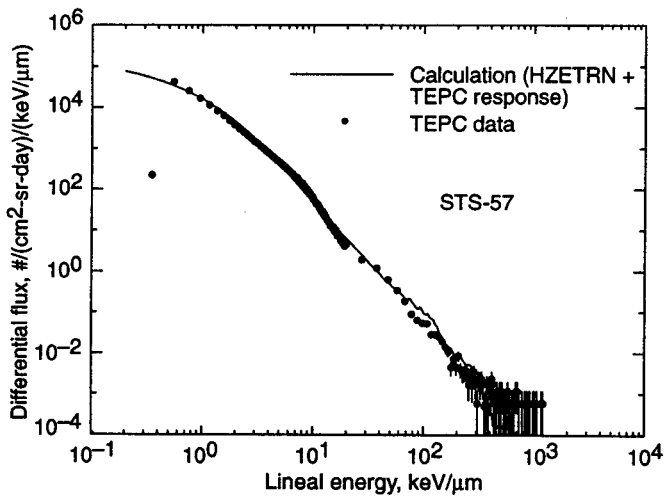

(b) Trapped protons

Figure 6. Comparison of differential lineal energy spectra with TEPC data for a 28-degree Shuttle flight.

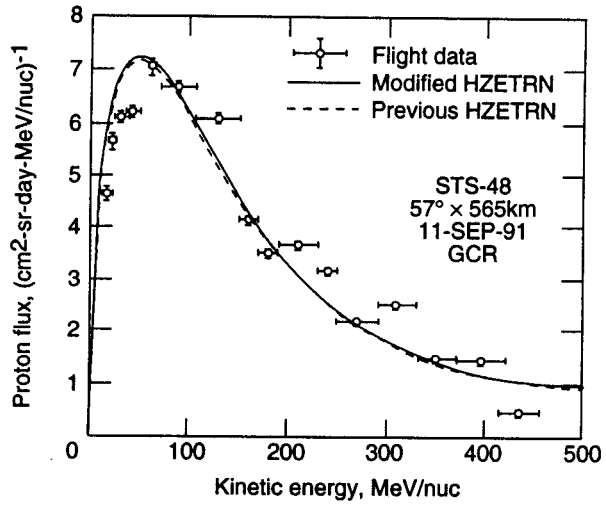

Figure 7. Differential energy spectra of secondary protons produced by GCR particles for STS-48.

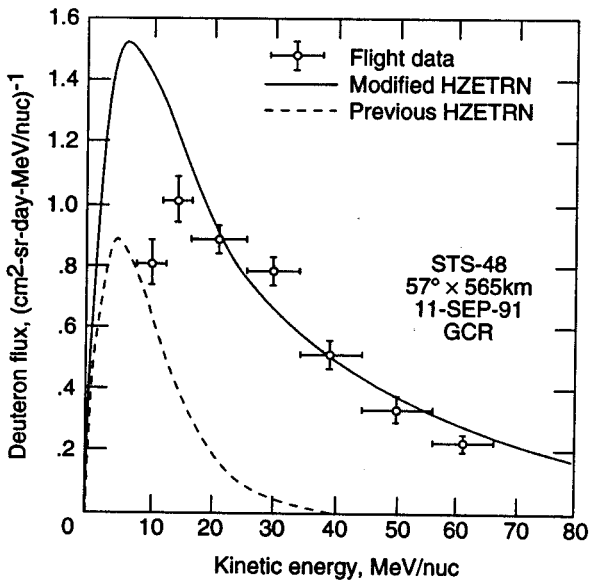

Figure 8. Differential energy spectra of secondary deuterons produced by GCR particles for STS-48.

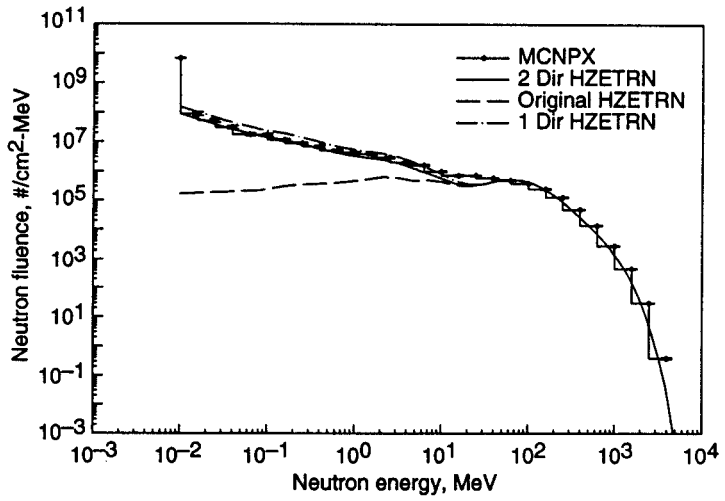

Figure 9. Energy spectra of neutron fluences at 30-g/cm^2 depth of water behind 100 g/cm^2 aluminum slab exposed to February 1956 solar flare, as calculated using original and improved (1-directional and 2-directional) HZETRN and Monte Carlo (MCNPX) code. The water slab is assumed to be 100 g/cm^2 in thickness.